



**Public
Report**

Document ID 1206894	Version 1.0	Status Approved	Reg no	Page 1 (27)
Author Lennart Börgesson/Clay Technology AB Lars-Erik Johannesson/Clay Technology AB Heikki Raiko/VTT			Date 2009-08-27	
Reviewed by			Reviewed date	
Approved by Håkan Rydén			Approved date 2009-12-08	

Uneven swelling pressure on the canister simplified load cases derived from uneven wetting, rock contours and buffer density distribution

Abstract

A number of different load cases that may be harmful for the canister have been investigated. Such load cases are derived from uneven swelling pressure in the buffer material, both during the water saturation phase and after full water saturation. Different cases are critical for the cast iron insert and the copper shell. Simple interpretations of those data and addition of cases may yield unrealistic and thus conservative load cases. No evaluation of the quality and probability of the load cases have been done. Three main types of stress combinations have been considered.

Remaining stresses which after full water saturation of the buffer are critical to the cast iron insert

The load cases regarding permanent stresses in the buffer that are critical for the cast iron insert are derived from uneven horizontal stresses where the canister acts as a freely supported beam. The worst case that may occur if requirements on the buffer and deposition hole are fulfilled combines a banana shaped hole and a local rock fall out of 3.75% of the cross section area. Simplified calculations of the stresses in the canister insert yield to a maximum bending stress $\sigma_b = 111.5$ MPa.

Revisionsförteckning

Version	Date	Description	Author	Reviewed	Approved
1.0	Se sidhuvud	New report	Se sidhuvud	Enligt SKB-doc 1213590	Se sidhuvud

Temporary stresses during the water saturation phase of the buffer that are critical to the cast iron insert

These load cases that concern temporary stresses are also derived from uneven horizontal stresses where the canister acts as a freely supported beam. The worst case that may occur if requirements on the buffer and deposition hole are fulfilled is a banana shaped hole. Simplified calculations of the stresses in the canister insert yield to a maximum bending stress $\sigma_b = 105$ MPa.

This load case is the result of simplified assumptions during the complicated wetting phase and is probably conservative.

Remaining stresses after full water saturation of the buffer that are critical to the copper shell

The most critical stresses on the copper shell may proceed from uneven vertical stresses caused by vertical density gradients in the buffer, which causes shear stresses on the copper. The worst case comes from a high buffer density of Ca converted MX-80 in the bottom of the deposition hole in combination with unconverted MX-80 in the upper part and the highest possible axial density gradient caused by rock fallout. This case yields axial shear stresses on the copper shell that is linearly reduced from $\tau = 2.55$ MPa to $\tau = 0.573$ MPa over the length 1.96 m.

The complicated nature of these load cases calls for more relevant finite element calculations if the stresses are considered critical.

Sammanfattning

Ett flertal lastfall som kan vara skadliga för kapseln har undersökts. Sådana lastfall uppkommer av ojämna svälltryck i buffertmaterialet, både under vattenmättnadsfasen och efter full vattenmättnad. Förenklad utvärdering av data och addition av laster kan ge orealistiska och konservativa lastfall. Olika fall är kritiska för gjutjärnsinsatsen och kopparhöljet. Tre huvudtyper av lastkombinationer har beaktats.

Kvarstående spänningar som efter full vattenmättnad av bufferten är kritiska för stålinsatsen

Lastfallen som avser kvarstående spänningar i bufferten som är kritiska för gjutjärnsinsatsen, härrör från ojämna svälltryck mot kapseln då kapseln fungerar som en fritt upplagd balk. Det värsta fallet som kan inträffa, om kraven på bufferten och deponeringshål är uppfyllda, är en kombination av ett bananformat hål och ett lokalt bergutfall av 3.75% av tvärsnittsytan. Förenklade beräkningar av spänningarna i kapselinsatsen ger en maximal böjspänning av $\sigma_b = 111.5$ MPa.

Tillfälliga spänningar i bufferten som under vattenmättnadsfasen är kritiska för stålinsatsen

Dessa lastfall som rör tillfälliga spänningar uppkommer också av ojämna horisontella svälltryck mot kapseln där kapseln fungerar som en fritt upplagd balk. Det värsta fallet som kan inträffa, om kraven på buffert och deponeringshål är uppfyllda, är ett bananformat hål. Förenklade beräkningar av spänningarna i kapselinsatsen ger för detta fall en maximal böjspänning $\sigma_b = 105$ MPa.

För detta lastfall har förenklade antaganden om den komplicerade bevättningsfasen gjorts, vilket medför att resultaten antagligen är konservativa.

Kvarstående spänningar som efter full vattenmättnad av bufferten är kritiska för kopparhöljet

De mest kritiska spänningarna på kopparhöljet kan uppkomma av ojämna vertikala spänningar orsakade av en densitetsgradient i bufferten, som ger skjuvspänningar mot kapseln. Det värsta lastfallet härrör från en hög buffertdensitet hos Ca-konverterad MX-80 i botten på deponeringshållet i kombination med okonverterad MX-80 i den övre delen och största möjliga axiella densitetsgradient orsakad av bergutfall. Detta fall ger axiella skjuvspänningar på kopparhöljet som reduceras linjärt från $\tau = 2.55$ MPa till $\tau = 0.573$ MPa över längden 1.96 m.

Den komplicerade beskaffenheten hos dessa lastfall gör att mer relevanta finita-element-beräkningar behöver göras om spänningarna anses kritiska för kapseln.

Contents

1	Introduction	5
2	Remaining stresses after full water saturation of the buffer that are critical to the cast iron insert	6
2.1	General	6
2.2	Load cases	6
2.3	Rock contour unevenness	10
2.4	Resulting stress distribution	11
2.5	Calculation of stresses in the canister	14
3	Temporary stresses during the water saturation phase of the buffer that are critical to the cast iron insert	16
3.1	General	16
3.2	Load case	16
3.3	Rock contour unevenness and resulting stress distribution	18
3.4	Calculation of stresses in the canister	19
3.5	Comments	20
4	Remaining stresses after full water saturation of the buffer that are critical to the copper shell	21
4.1	General	21
4.2	Load cases	21
4.3	Comments	25
5	Conclusions and comments	26
6	References	27

1 Introduction

In addition to the shear load caused by slip in a fracture intersecting a deposition hole at an earth quake, there are a number of different load cases that may be harmful for the canister. Such load cases are derived from uneven swelling pressure in the buffer material, both during the water saturation phase and after full water saturation.

The swelling pressure on the canister after full water saturation and homogenisation is usually considered to be homogeneously acting on the canister, but due to unevenness in the rock contour and variation in geometry and density of the buffer blocks there may be considerable uneven loads on the canister that may remain for long time and contribute to the high stresses in the canister. The homogenisation will not be complete due to friction in the bentonite that keeps the density differences intact for long times. Permanent uneven swelling pressure may thus remain on the canister. Completely different load cases are critical for the cast iron insert and the copper shell.

Also during the water saturation phase of the buffer uneven swelling pressure may occur on the canister due to uneven wetting from the rock. If the uneven wetting is combined with unfavourable geometry of the deposition hole significant stresses may occur in the canister.

In order to try to find out how high such stresses can be in the most unfavourable cases the following three types of stresses have been investigated:

1. Remaining stresses after full water saturation that are critical to the cast iron insert
2. Temporary stresses during the water saturation phase that are critical to the cast iron insert
3. Remaining stresses after full water saturation that are critical to the copper shell

This report is a load definition report and the stress estimates made here are only indicative and made for ranking various load cases. The actual stress calculations and the assessment of acceptability are made later in separate report using 3D-FEM-modelling and taking into account shear deformation, large displacements and non-linear material properties.

Due to the fact that SKB has not yet defined acceptance criteria for deposition holes are the irregularities that may occur in the contour of the deposition hole taken from the Underground openings construction report /SKB, 2009b /, Buffer production report /SKB, 2009a / and a report on experiences from the deposition hole boring in Äspö /Andersson et al. 2002/. When SKB has set the acceptance criteria the simple interpretations of these data and definition of various load cases in this report may yield over conservative and having a low-, or very low probability. However, for estimation purposes the defined “worst case scenarios” defined in this report can be used as the upper limit for the loads on the canister.

2 Remaining stresses after full water saturation of the buffer that are critical to the cast iron insert

2.1 General

Due to unevenness and geometrical variations in the rock contour and variation in geometry and density of the buffer there may be considerable uneven loads on the canister after completed water saturation and swelling of the buffer, since friction in the bentonite prevents complete homogenisation.

2.2 Load cases

Since the canister is about 5 times longer than the diameter it may in a simplified way be considered a beam and the worst load case for the cast iron insert would correspond to the worst load case of a beam.

A number of load postulations that are statically reasonable have been analysed in this way and the worst case from the bending stress point of view is a freely supported beam loaded by limited pressure load areas as shown in Figure 2-1. The vectorial sum of the load shall always be zero in static condition.

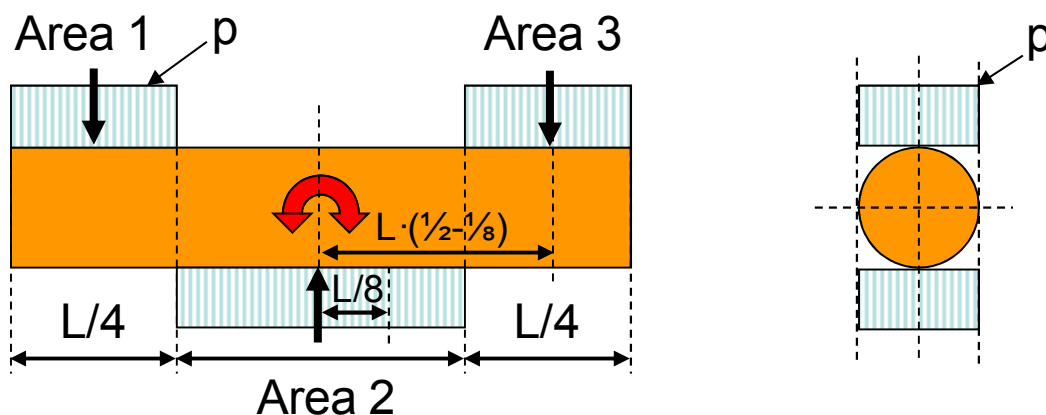


Figure 2-1. Worst load case of uneven remaining swelling pressure on the canister with the canister tilted 90 degrees in order to illustrate the case of a freely supported beam

This load case may with conservative assumptions be achieved at a very unfavourable stress distribution, whereby the net swelling pressure (difference in swelling pressure acting on opposite sides) may occur along the areas 1 – 3. The load is assumed conservatively to be a pressure acting with same maximum power on half of the circumference (180 degrees), see Figure 2-4, and it is equivalently modelled as a constant projected distributed load of the width $= D$ on the beam. This projection means that the component of the pressure perpendicular to the canister axis acting on the cylindrical surface is taken into account. The axial component does not need to be taken into account, because the sum of that is zero due to symmetry. The following basic values can be applied:

$L = 4.8$ m (length of canister)

$D = 1.05$ m (diameter of canister)

p = net swelling pressure (MPa) according to Equation 2-9

We can get **an indicative estimate of the stress level** in the insert by doing a simplified stress analysis according to classical Euler-Bernoulli beam theory. The reference canister is modelled as a beam that is loaded by the distributed load described in Figure 2-1. The distributed load density along the length of the canister is $q(x) = p(x) \cdot D$, where p is the pressure-difference caused by variation in the bentonite properties or geometry at position x and D is the diameter of the canister shell. The effect of the load-bearing capacity of the copper shell is ignored in this indicative estimate. The estimate is done only to get advance information about the effects of the uneven swelling pressure. **The actual stress calculations and the assessment of acceptability are made later in separate report using 3D-FEM-modelling and taking into account shear deformation, large displacements and non-linear material properties.**

According to beam theory, the load density $q(x)$ is

$$q(x) = E \cdot I \cdot d^4 u / dx^4 \quad (2-1)$$

where E is Young's modulus, I is the second moment of area (= moment of inertia) of the beam section, u is the deflection of the beam and x is the longitudinal coordinate along the beam axis. Notation $d^4 u / dx^4$ means the fourth derivative of the deflection u in relation to axial coordinate. Further according to beam theory, the shear force $Q(x)$ in the beam is

$$Q(x) = - E \cdot I \cdot d^3 u / dx^3 \quad (2-2)$$

where $d^3 u / dx^3$ means the third derivative of the deflection u in relation to axial coordinate. Further, by integrating, we get the bending moment $M(x)$ in the beam

$$M(x) = - E \cdot I \cdot d^2 u / dx^2 \quad (2-3)$$

where $d^2 u / dx^2$ means the second derivative of the deflection u in relation to axial coordinate.

Now $q(x)$ is known according to Figure 2-2, E is a material constant and I is a geometrical constant of the section. By integrating the load density $q(x)$ we get the shear force $Q(x)$, and further, by integrating the shear force $Q(x)$ we get the bending moment $M(x)$. The phases of the integration process are shown in Figure 2-2. The maximum bending moment is obtained at the centre of the beam length L , where the shear force $Q(x) = 0$. The maximum bending moment $M_{max} = p \cdot D \cdot L^2 / 16$.

At location of maximum bending moment the shear force is zero, because shear force is the derivative of the bending moment function. Thus the omitting of the shear stress in the comparison does not lead into remarkable error in assessing the maximum combined stress only by bending stresses.

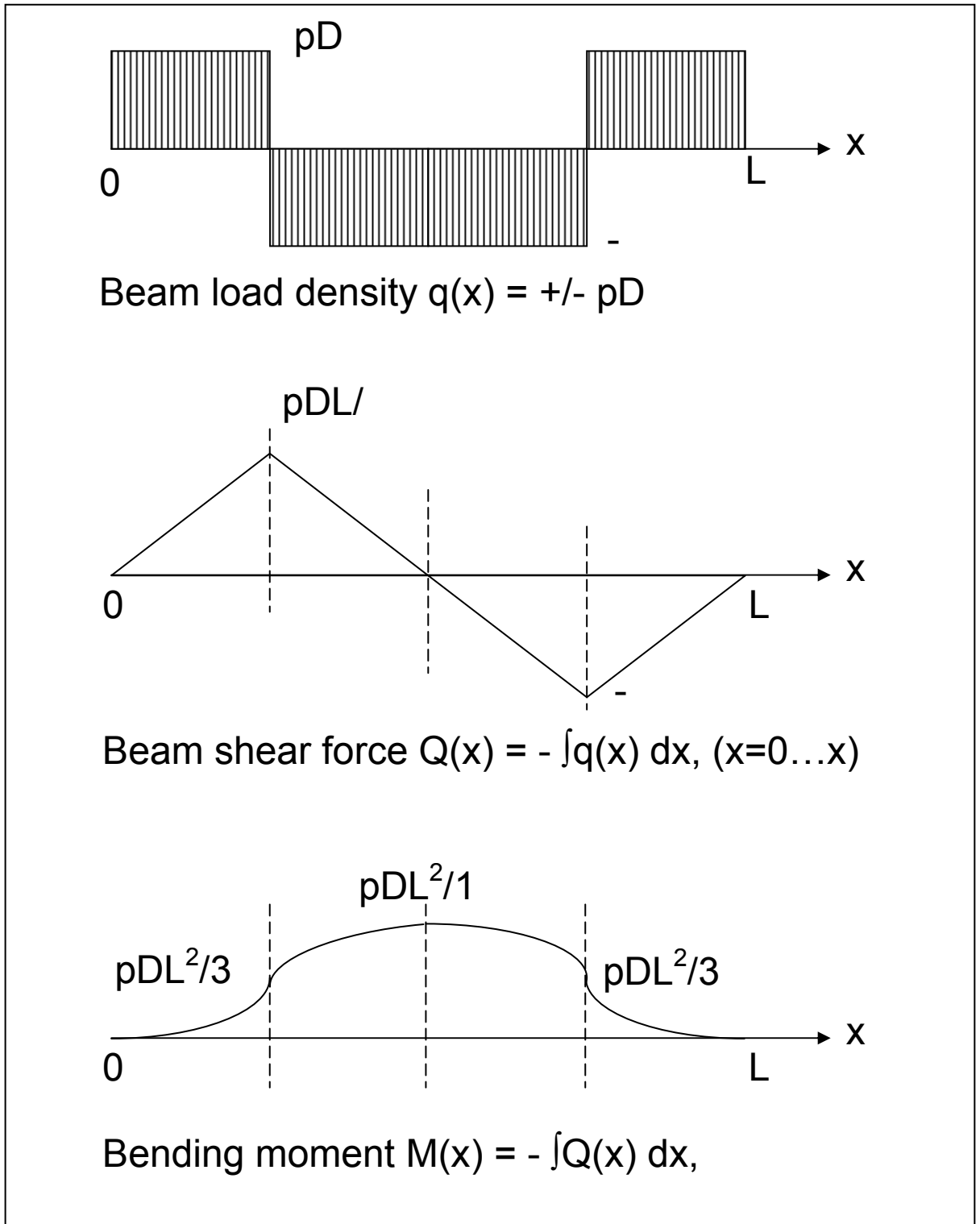


Figure 2-2. The derivation of bending moment from beam load density by integration

To get an idea of the bending stress at the insert, we have to calculate the section modulus (W) of the insert. Easiest way to define W is first to calculate the second moment of area (I) (or moment of inertia) of the beam section. Moment of inertia I_z for the insert section is calculated from basic handbook solutions for circular and square sections as follows:

$$I_z (\text{circle}) = \pi \cdot r^4 / 4 \quad (2-4)$$

and

$$I_z (\text{square}) = h^4 / 12 \quad (2-5)$$

where r is the radius of the circle ($r = 0.949/2 = 0.4745$ m) and h is the side length (160 mm) of the square opening. For BWR-type insert the moment of inertia in relation to neutral axis z is the circular I_z of the insert cylinder subtracted by the 12 square openings. When subtracting the effect of openings, we have to consider also the effect of the distance of the openings from the neutral axis by using the Steiner's rule. The moment of inertia of the BWR-insert is

$$I_z (\text{BWR}) = \pi \cdot r^4 / 4 - [12 \cdot (h^4 / 12) + 8 \cdot h^2 \cdot e_1^2 + 4 \cdot h^2 \cdot e_2^2] \quad (2-6)$$

where e_1 and e_2 are the distances of the centres of the 8 closer and 4 farther square openings from the neutral axis. The distances e_1 and e_2 are according to Figure 2-3 are 105 mm and 315 mm in case of BWR-insert and the e_1 distance is 185 mm in case of PWR insert. Axis A-A in both sections in Figure 2-3 is the neutral axis due to symmetry. The moment of inertia is calculated accordingly for PWR-type insert, taking into account that there are only 4 openings and that they all have the same distance from the neutral axis. We get $I_{z \text{ BWR}} = 0.026740 \text{ m}^4$ and $I_{z \text{ PWR}} = 0.031237 \text{ m}^4$.

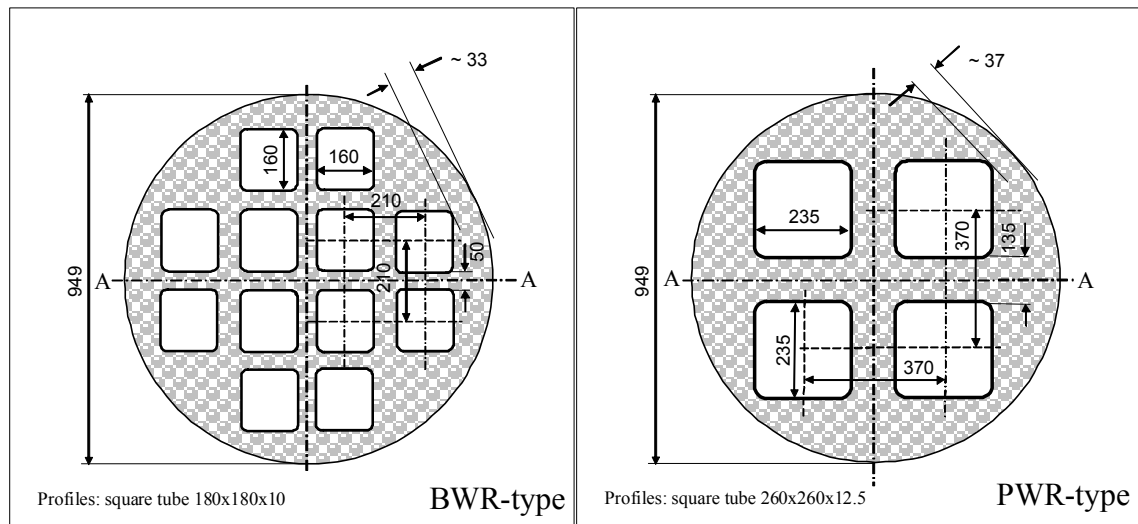


Figure 2-3. The geometry and dimensions of the two insert sections

Bending stress σ_b in a beam is calculated from bending moment M and moment of inertia I_z as follows

$$\sigma_b = M \cdot y / I_z = M / W \quad (2-7)$$

where M is the bending moment, y is the distance from neutral axis and I_z is the moment of the inertia of the beam section. I_z / y is also commonly called as the sectional modulus and its symbol is W . In inserts the maximum distance $y = r = 0.4745$ m.

Thus we get $W_{BWR} = 0.05635 \text{ m}^3$ and $W_{PWR} = 0.06583 \text{ m}^3$.

With these data the maximum bending moment M will be

$$M = p \cdot L^2 \cdot D / 16 = p \cdot 1.51 \text{ m}^3 \quad (2-8)$$

which yields to the maximum bending stress σ_{max} according to Equation 2-7 on the surface of the insert:

There are of course counter pressure (or supporting reaction) in the opposite side of the canister but Figure 2-1 only shows the net pressure. Due to unevenness in the rock contour the space between the canister and the rock surface may differ and the results will be a difference in density and resulting local difference in swelling pressure at opposite sides of the canister.

2.3 Rock contour unevenness

There are several factors that may affect the rock contour after drilling of the bore hole. The most important ones are the following:

- The inclination of the hole may differ from vertical
- The deposition hole is curved (banana shaped)
- There may be rock fall out caused by e.g. spalling
- There may be a change in diameter due to change of bore crown etc

Since the load case is only sensitive to factors that cause a difference in buffer density at the same horizontal section of a deposition hole a change in borehole diameter will not cause loads like the case described. Neither will an inclined deposition hole since it will only make the canister tilt. There must be force equilibrium in horizontal direction, which means that a rock fall out on one side of the deposition hole is not severe since the canister will get displaced or tilt unless the rock fallout is local at the central part of the canister.

Two cases may yield a stress distribution that is similar to the one shown in Figure 2-1:

Case 1: Banana shaped deposition hole

Case 2: Rock fall out at critical locations

The two severe cases are thus a banana shaped deposition hole with rock fallout at places that accentuate the shape as illustrated in Figure 2-4.

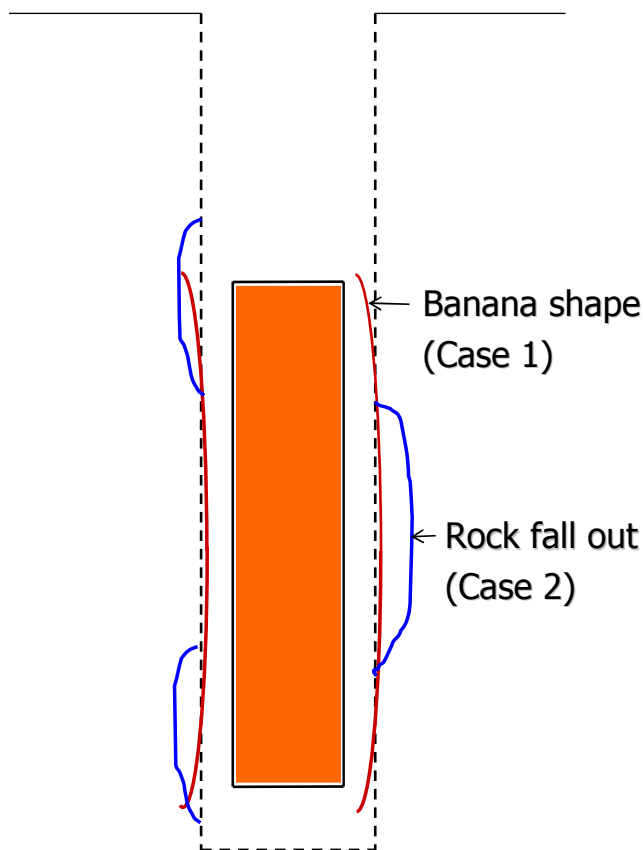


Figure 2-4. Two severe cases of deformed rock contours. The red lines illustrate a banana-shaped hole and the blue lines illustrate rock fallouts that accentuate the banana shape.

2.4 Resulting stress distribution

The combined cases in Figure 2-4 can be simplified with the load case illustrated in Figure 2-1 by simplifying the rock contour caused by the two cases as shown in Figure 2-5. The rock surface is assumed to be vertical with a distance to the canister surface that corresponds to the average distance over a quarter of the canister length at the top and bottom of the canister and over half the canister length in the centre of the canister. These lengths are chosen to yield force equilibrium in horizontal direction.

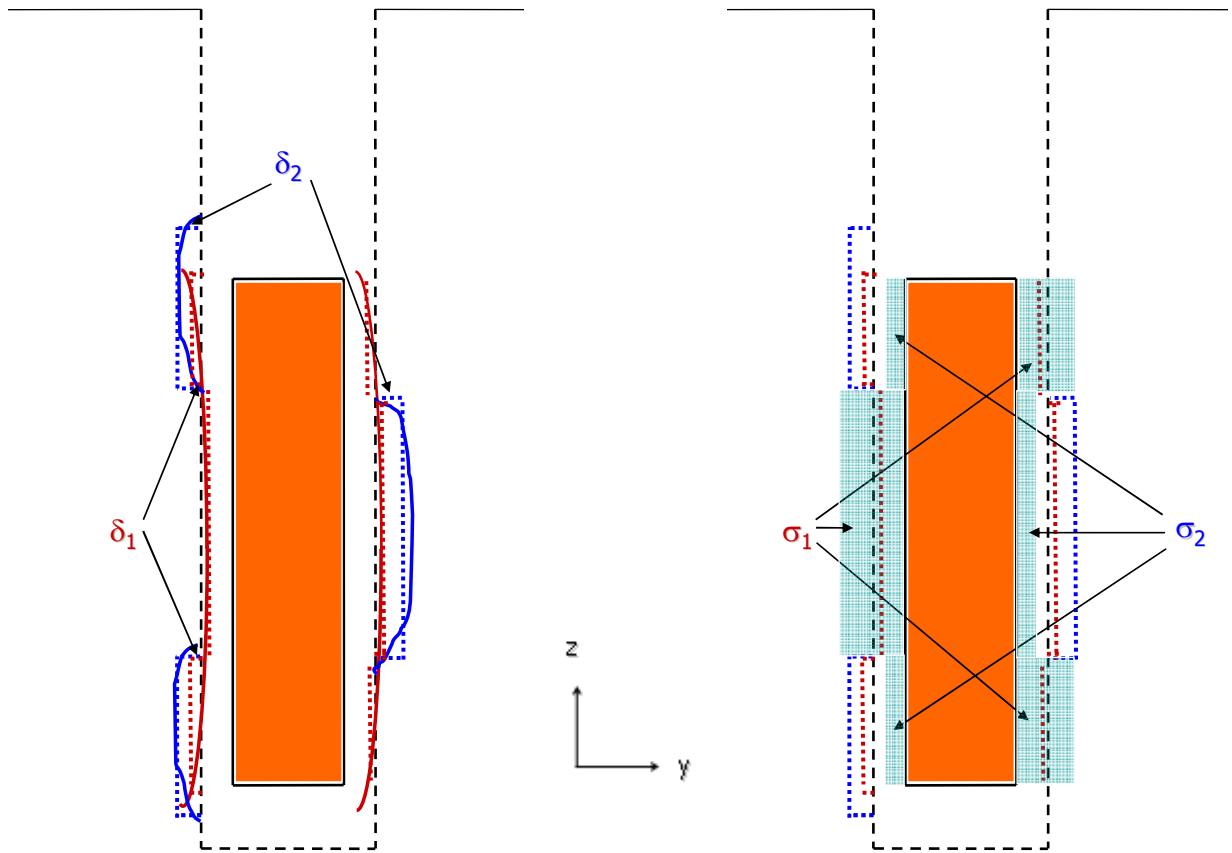


Figure 2-5. Simplified rock contours in a vertical cross section marked with dotted lines (left) and resulting swelling pressure on the canister marked as blue areas (right). δ_1 and δ_2 correspond to the average deviation from nominal distance between the rock and the canister surface caused by the banana shape and the rock fallout respectively. σ_1 and σ_2 correspond to the resulting swelling pressure of the combined effects.

δ_1 =deviation in distance due to the banana shape
 δ_2 =increased distance due to rock fall out

An increased distance yields a decreased swelling pressure since the mass of bentonite is the mass in the bentonite ring plus the mass of pellets between the bentonite ring and the rock surface. Since the density of the pellets filling is much lower than the average density an increased distance will yield a decreased average density and thus decreased swelling pressure. Figure 2-5 only shows the cross section but the geometry is 3-dimensional so the geometry and resulting swelling pressure distribution is assumed to act on half the canister in a horizontal cross section according to Figure 2-6.

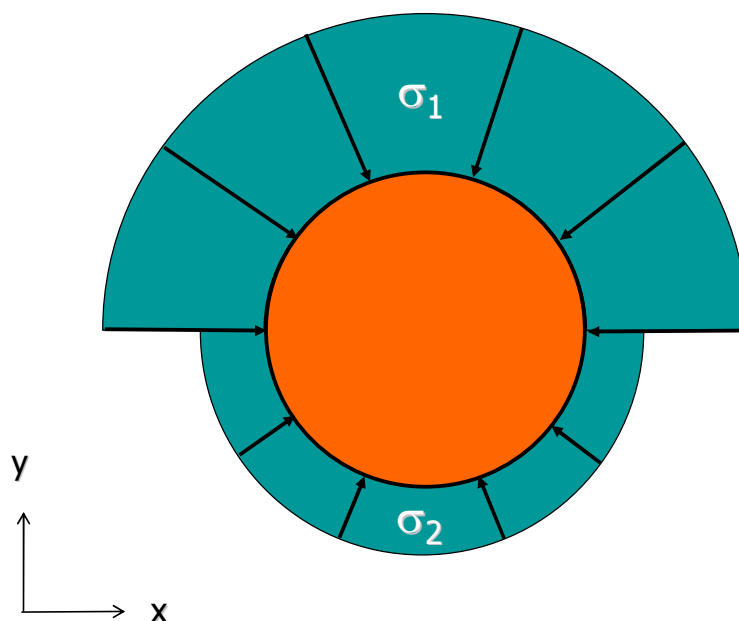


Figure 2-6. Simplified swelling pressure distribution in a horizontal cross section

Since the swelling pressure is close to isotropic the resulting bending load around the most stressed direction (y-direction in Figures 2-5 and 2-6) can be simplified as a constant distributed load with the width D (that equals to projection of the actual pressure on a cylindrical surface) as shown in Figure 2-1.

A relation between swelling pressure and density that can be used for evaluating σ_1 and σ_2 is needed. For the calculations described in this report the following relation between void ratio and swelling pressure has been used /Börgesson et al, 1995/:

$$\sigma = \sigma_0 \left(\frac{e}{e_0} \right)^{\frac{1}{\beta}} \quad (2-9)$$

e = current void ratio

e_0 = reference void ratio (=1.1)

σ = current swelling pressure

σ_0 = swelling pressure at e_0 (= 1000 kPa for MX-80)

β = -0.19

The void ratio e can be calculated from the density at saturation with equation 2-10:

$$e = (\rho_s - \rho_m) / (\rho_m - \rho_w) \quad (2-10)$$

ρ_m = density at water saturation

ρ_s = density of solids = 2 780 kg/m³

ρ_w = density of water = 1 000 kg/m³

Equation 2-9 is based on measurements on MX-80 from 1995. Later measurements have confirmed these data but also shown that there is a scatter and that there is an influence of external factors such as a history of swelling, very high water pressure and ion-exchange from Na to Ca. The data used refer to the normal case.

2.5 Calculation of stresses in the canister

The stresses in the canister have been calculated in the following way:

1. The worst cases of deformed rock contour shown in Figure 2-4 have been evaluated according to Figures 2-5 and 2-6.
2. The maximum deviation in distance between the canister and the rock from the nominal value 355 mm has been set according to acceptance criteria for each case
3. The resulting density of the buffer caused by the mentioned deviation has been calculated
4. The expected swelling pressure at the resulting density has been calculated according to Equation 2-9
5. The resulting net swelling pressure $p = \sigma_1 - \sigma_2$ has been used and put into Equation 2-8
6. The maximum bending moment M_{max} and the maximum stress in the canister σ_{max} have been calculated according to Equations 2-8 and 2-7

The basic geometry and density data are the following:

Geometry:

Canister radius $r = 525$ mm

Slot between canister and bentonite ring $\Delta r = 10$ mm

Bentonite ring $\Delta r = 280$ mm

Pellets filled slot $\Delta r = 60$ mm

Deposition hole radius $r = 875$ mm

Density:

Bentonite ring $\rho = 2070$ kg/m³; $w = 17.0\%$

Pellets filled slot $\rho = 1100$ kg/m³; $w = 10.0\%$

where

ρ = bulk density (dry mass + mass of water divided by volume)

w = water content (mass of water divided by dry mass)

The following cases have been considered (see Figure 2-5):

- Case 1: Banana-shaped hole with $\delta_1 = 8$ mm on both sides of the canister
- Case 2: Rock fallout with 3.75% (corresponding to half of the maximum allowed volume 7.5 %) rock lost on different sides of the canister. This yields a local increase in radius of $\delta_2 = 33$ mm on one side with lengths and locations according to Figure 2-5. 2.5 mm smaller radius is assumed on the other side, which is the maximum allowed reduction in deposition hole radius (caused by tear-and-wear of the crown).
- Cases 1+2: Combination of Case 1 and 2a so that these coincide to create the worst possible case.

The values of the maximum allowed banana shape 8 mm, the maximum allowed rock fallout 7.5% (outside the nominal radius) and the tear-and-wear allowance of the crown 5 mm are evaluated from the Underground openings construction report /SKB, 2009b /, Buffer production report /SKB, 2009a / and experiences from the deposition hole boring in Äspö /Andersson et al. 2002/.

The results of the calculations are shown in Table 2-1.

Table 2-1. Stresses in the canister at different load cases

Case	Width of pellets filled slot	Slot width mm	e	ρ_m kg/m ³	σ_1/σ_2 kPa	M_{max} MNm	σ_{max} MPa
Case 1	Banana shaped $\delta_l=8$ mm						
	Pellets filled slot (σ_2): 60 mm+8 mm	68	0.787	1996	5832		
	Pellets filled slot (σ_l): 60 mm-8 mm	52	0.750	2017	7503	2.563	45.49
Case 2	Rock fallout (3.75% increased area on one side) $\delta_2=33$ mm						
	Pellets filled slot (σ_2): 60 mm+33 mm	93	0.840	1967	4122		
	Pellets filled slot (σ_l): 60 mm-2.5 mm	57.5	0.763	2010	6860	4.201	74.56
Cases 1+2							
	Pellets filled slot (σ_2): 60 mm+41 mm	101	0.857	1959	3727		
	Pellets filled slot (σ_l): 60 mm-10.5 mm	49.5	0.744	2021	7823	6.284	111.5

Shear stresses are analyzed as well. As first approximation, the shear stress is considered the same in all section. The maximum shear stress is in the BWR canister, which has a section area of 0.4 m².

Case 1+2 is the worst case, so the $Q_{max} = 5.16$ MN and the shear stress $\tau = 12.91$ MPa.

In the section where there is the maximum shear stress there is also a bending stress (see Figure 2-2). The bending moment is $M = 3.1$ MNm and the maximum stress σ_b is 58.04 MPa.

The yield criteria usually considered in steel is the Von Mises model. For case of bending plus shearing, the stress σ_{CO} to compare with the yield stress is $\sigma_{CO} = \sqrt{\sigma^2 + 3 \times \tau^2}$. In this case, $\sigma_{CO}=62.8$ MPa, which is less than 111.5 MPa, (the maximum in the center of the canister, where the shear stress is 0) so the section with maximum shear stress is not the critical section.

The dimensioning case (1+2) yields the indicative bending stress 111.5 MPa, which is less than half of the yield stress of the iron insert ($\sigma_y = 270$ MPa in tension).

3 Temporary stresses during the water saturation phase of the buffer that are critical to the cast iron insert

3.1 General

During the water saturation phase of the buffer in a deposition hole uneven swelling pressure may occur on the canister due to uneven wetting from the rock. If the uneven wetting is combined with unfavourable geometry of the deposition hole significant stresses may occur in the canister.

3.2 Load case

The same type of load cases may occur during the wetting phase as after full saturation and the worst case is the same with a freely supported beam loaded by limited pressure load areas as shown in Figure 3-1. The vectorial sum of the load shall always be zero in static condition.

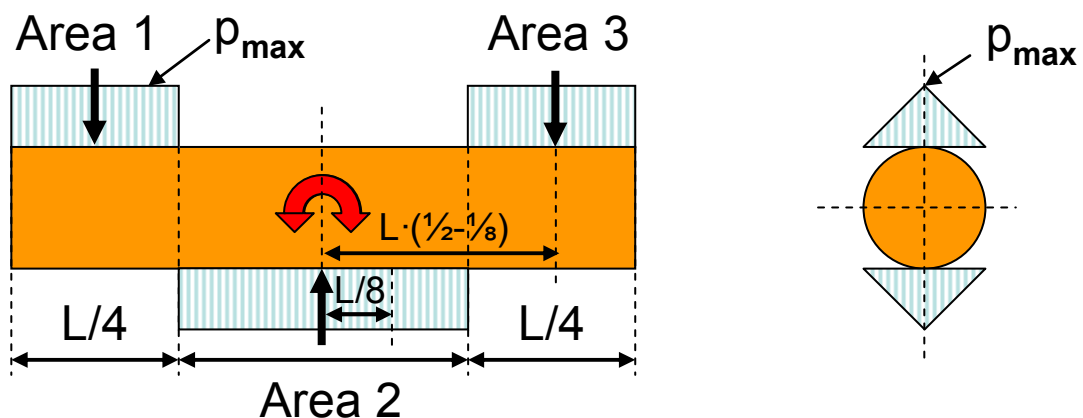


Figure 3-1. Worst load case of uneven temporary swelling pressure on the canister with the canister tilted 90 degrees in order to illustrate the case of a freely supported beam

The stress distribution is in this case not rectangular but triangular since water is assumed to be available from vertical fractures and the wetting and generated swelling pressure will on this reason change with distance from the fracture. Figure 3-2 illustrates how the wetting distributes from a vertical fracture and the resulting swelling pressure will (along the canister periphery) decrease with increasing distance from the fracture. If the wetting continues the swelling pressure will also act on the other side of the canister opposite to the fracture, which will reduce the net stress. A linear decrease in swelling pressure as shown in Figure 3-1 is therefore assumed to be the worst case. The actual shape is not known but a distribution similar to the triangular is a best estimate. The same distribution will probably occur also in axial direction but has not been considered, which is conservative.

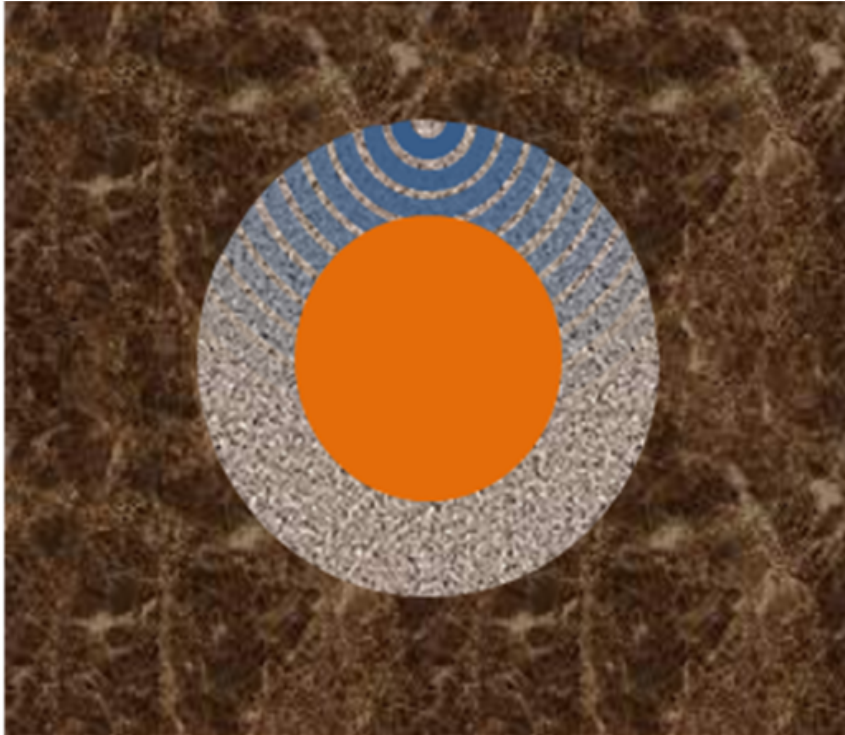


Figure 3-2. Illustration of the wetting from an axial fracture intersecting the deposition hole. The wetting and resulting swelling pressure decreases with distance from the fracture.

This load case may with conservative assumptions be achieved at very unfavourable wetting, whereby full swelling pressure may occur at the fractures along the water feeding areas 1 – 3, shown in Figure 3-1. This projection means that the component of the pressure perpendicular to the canister axis acting as a triangular load on cylindrical surface is considered. The axial component does not need to be taken into account, because the sum of that is zero due to symmetry. The following basic values can be applied:

$L = 4.8$ m (length of canister)

$D = 1.05$ m (diameter of canister)

$W_{insert} = 0.05635$ m³ (section modulus for BWR insert, the modulus for PWR is higher)

P_{max} = max swelling pressure (MPa)

The bending moment is calculated from the beam load density function in the same manner as in Chapter 2. The only difference is that the pressure load distribution in circumferential direction is assumed to be a triangle instead of the rectangle assumed in Chapter 2. With these data the maximum bending moment M will be

$$M = p_{max}/2 \cdot L/4 \cdot D \cdot L \cdot \{(\frac{1}{2} - \frac{1}{8}) - \frac{1}{8}\} = p_{max} \cdot L^2 \cdot D/32 = p_{max} \cdot 0.756 \text{ m}^3 \quad (3-1)$$

which yields the maximum bending stress σ_{max} on the surface of the insert:

$$\sigma_{max} = M/W = p_{max} \cdot 13.42 \quad (3-2)$$

Since the load case refers to the wetting case the worst case is that there is no counter pressure (or supporting reaction) in the opposite side of the canister. Due to unevenness in the rock contour, the space between the canister and the rock surface may differ and the results will be a difference in density resulting in higher density at the wetting lines at the most unfavourable case.

3.3 Rock contour unevenness and resulting stress distribution

Since the load case (Figure 3-1) is identical to the case when full water saturation has occurred the same two hole geometries can be used as dimensioning cases:

Case 1: Banana shaped deposition hole

Case 2: Rock fall out at critical locations (not considered)

Figure 3-3 illustrates the resulting geometry and stress distribution (identical with Figure 2-3).

- Nominal distance between bentonite ring and rock surface (pellets filled slot) $\Delta r=60$ mm
- δ_1 =decreased distance due to the banana shape
- δ_2 =increased distance due to rock fall out

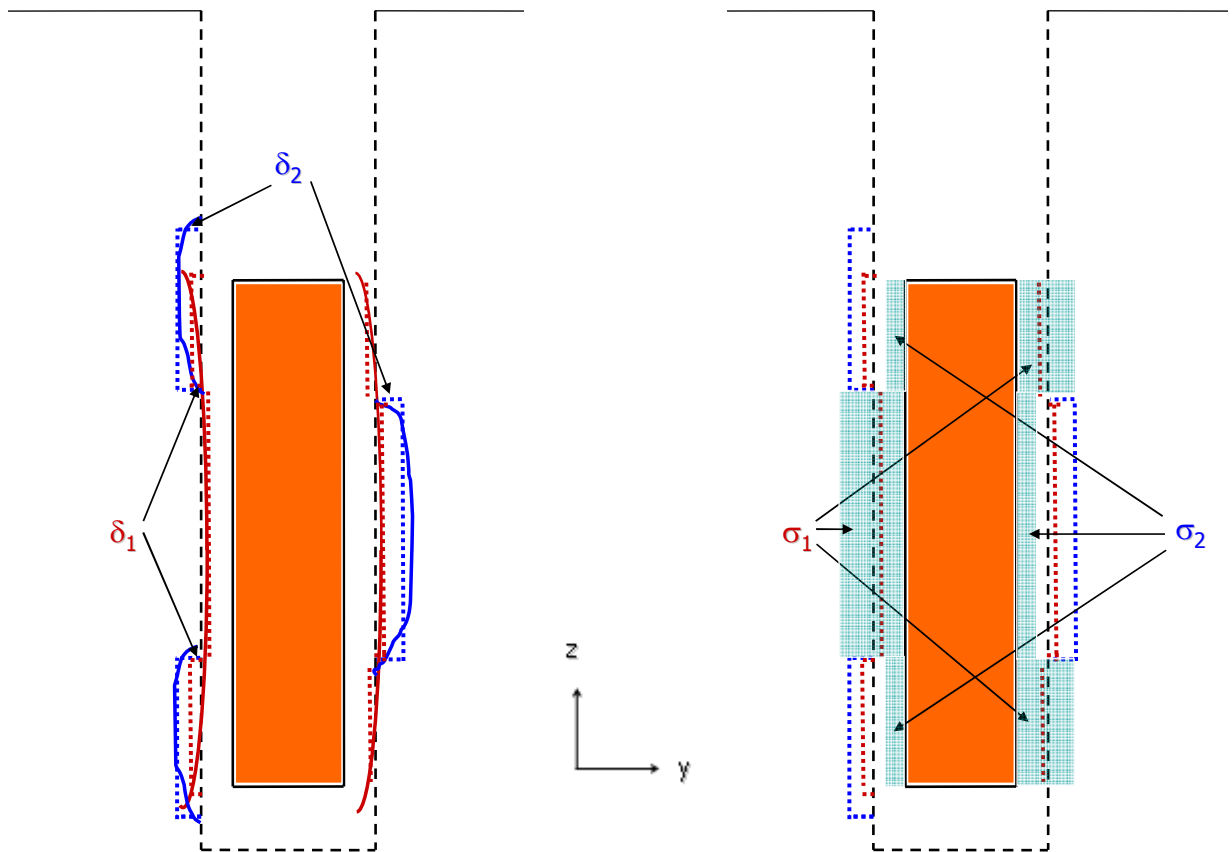


Figure 3-3. Simplified rock contours in a vertical cross section marked with dotted lines (left) and resulting swelling pressure on the canister marked as blue areas (right). δ_1 and δ_2 correspond to the average deviation from nominal distance between the rock and the canister surface caused by the banana shape and the rock fallout respectively. σ_1 and σ_2 correspond to the resulting swelling pressure of the combined effects. In this case $\sigma_2=0$.

The difference between the wetting case (this case) and the case after full water saturation is that in this case there is no counter pressure on the opposite sides of the canister, i.e. $\sigma_2=0$ and that case 2 rock fall out (δ_2) does not need to be considered since it only causes decreased density and swelling pressure.

The distance between the rock surface and the canister determines the resulting density and thus the swelling pressure, since the pellets filling has lower density than the average and the mass of bentonite is the mass in the bentonite ring plus the mass of pellets between the bentonite ring and the rock surface.

A relation between swelling pressure and density that can be used for evaluation σ_1 is needed where σ_1 is the swelling pressure at full water saturation. The same relations as in the previous chapter have been used (Equations 2-9 and 2-10) and the same density of solids and water.

3.4 Calculation of stresses in the canister

The stresses in the canister have been calculated in the same way as after full water saturation in chapter 2, with the exception that there is no counter pressure ($\sigma_2=0$).

The following cases have been considered (see Figure 3-3):

- Case 0: Nominal geometry and density with wetting according to Figure 3-1.
- Case 1: Banana-shaped hole with a reduced distance between the canister and the rock of $\delta_r = 8$ mm on the wetted periphery + 2.5 mm smaller hole radius due to the maximum allowed tear-and-wear of the crown.
- Case 2: Rock fall out. Not considered since it only causes decreased density and swelling pressure

The values of the maximum allowed banana shape 8 mm is taken from /Andersson and Johansson, 2002/.

The results of the calculations are shown in Table 3-1.

Table 3-1. Stresses in the canister at different load cases

Case	Width of pellets filled slot	Slot width mm	e	ρ_m kg/m ³	σ_1 kPa	M_{max} MNm	σ_{max} MPa
Case 0	Nominal geometry 60 mm slot and $\rho_m = 2006$ kg/m ³	60	0.769	2006	6594	4.985	88.46
Case 1	Banana shaped $\delta_r = 8$ mm Pellets filled slot: 60 mm-10.5 mm	49.5	0.744	2021	7823	5.914	105

The dimensioning case is thus case 1, which yields lower stresses than the worst case after full water saturation.

3.5 Comments

The load cases used for calculating the stresses in the canister have been derived through several simplifications that include a lot of uncertainties. The loads are assumed to be static without considering displacements and time scales. In the real case there is a complicated mechanical interaction between the bentonite and the canister that also includes the wetting rate. In order for the cases in Table 3-1 to appear not only the wetting areas but also time schedule and mechanical responses must interact in a precise way. In addition the consequences of the pellets filling on the wetting have not been considered. The pellets filling will under some circumstances spread the inflowing water along the rock surface due to the low flow resistance. The cases considered are thus rather unlikely.

4 Remaining stresses after full water saturation of the buffer that are critical to the copper shell

4.1 General

Different load cases are critical for the cast iron insert and the copper shell. While the worst stresses on the cast iron insert is caused by uneven horizontal swelling pressure the most critical stresses on the copper shell may proceed from uneven vertical swelling pressure. This difference is due to that horizontal stress differences that cause bending stresses are taken by the cast iron insert, while vertical stress differences may cause shear stresses along the copper shell that need to be taken by the copper.

The results of the presented calculations will be used as boundary conditions to analyse the stresses in the copper shell.

4.2 Load cases

The vertical stress differences that may cause the shear stresses along the copper shell originate from differences in bentonite density in vertical direction of the deposition hole.

Base case 1

One load case that may occur is that the density of the buffer in the bottom of the deposition hole exactly below the canister is $2\,050\text{ kg/m}^3$ and the density in the top of the deposition hole exactly above the canister is $1\,950\text{ kg/m}^3$. This case can be considered possible since there may be rock fall out in the upper parts and upwards swelling of the buffer against a dry backfill, which will cause a decrease in buffer density in the upper part. Figure 4-1 shows the assumed stress distribution on the surface of the canister for this load case.

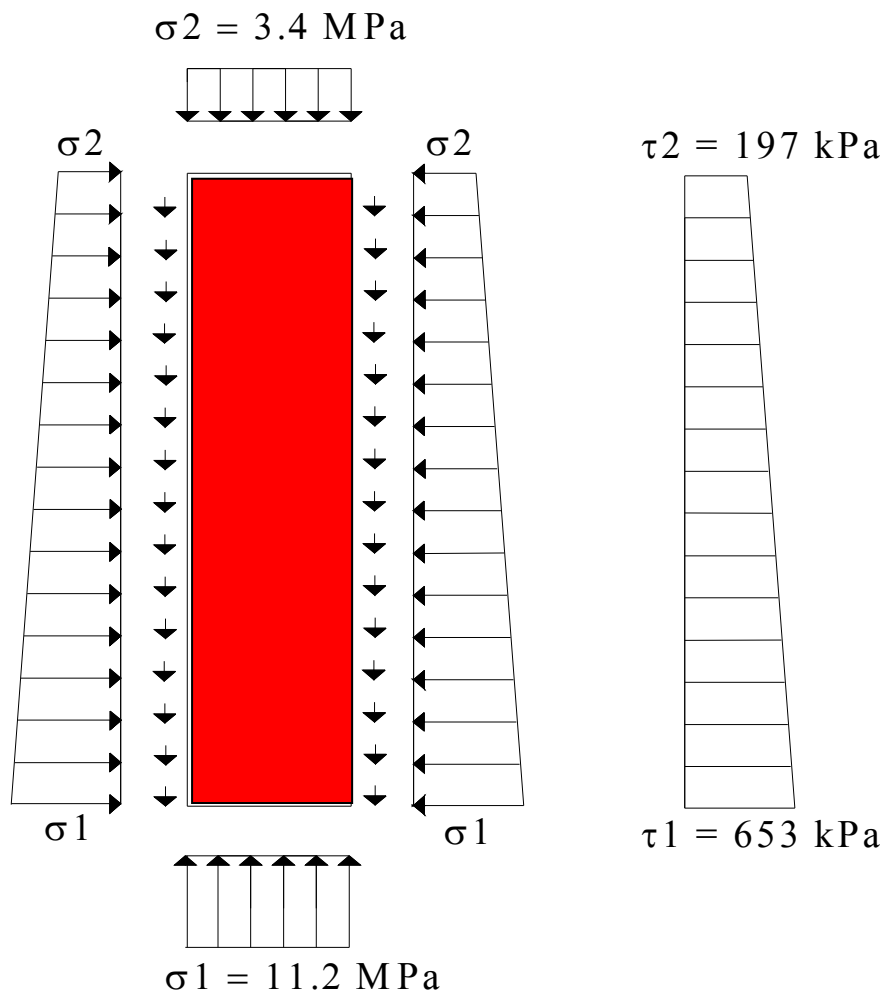


Figure 4-1. Base case 1. Normal stress on the canister surface and resulting shear stresses in the interface between the canister and the buffer for MX80.

The stresses shown in Figure 4-1 are derived in the following way:

The density at saturation in the top and the bottom of the canister is 1950 kg/m^3 and 2050 kg/m^3 , which result in the following swelling pressures for MX-80 (Equations 2-9 and 2-10).

$$\sigma_m = 2050 \text{ kg/m}^3 \rightarrow \sigma_j = 11.2 \text{ MPa}$$

$$\sigma_m = 1950 \text{ kg/m}^3 \rightarrow \sigma_j = 3.4 \text{ MPa}$$

Assuming that swelling pressure is linearly changed from the top of the canister to the bottom the shear stresses will be as described in Table 4-1 by applying force equilibrium to the canister.

Table 4-1. Calculation of vertical shear stresses on the canister surface for base case 1

Total force on the canister bottom	9 695.8 kN
Total force on the canister top	2 917.1 kN

The difference in force is taken by shear forces on the canister surface, which are generated by shear stresses proportional to the normal stresses

Total shear force	6 778.7 kN
Total horizontal (normal) force on the canister envelope surface	116 159 kN
Mobilized friction between the canister surface and the bentonite ($\tan\phi$)	0.0584
Shear stress in the top: $\tau_2 = \sigma_2 \cdot \tan\phi$	197 kPa
Shear stress in the bottom: $\tau_1 = \sigma_1 \cdot \tan\phi$	653 kPa

The mobilised friction between the canister surface and the bentonite 0.0584 corresponds to a friction angle of $\phi = 3.34^\circ$, which is lower than the friction angle at failure and can thus be mobilised.

Base case 2

A fictive case that may be considered is if the lower half of the buffer in the deposition hole is ion-exchanged to Ca (MX-80Ca). This could yield a swelling pressure in the bottom of 15 MPa /Börgesson et al, 2009/ while the swelling pressure in the top would remain. The results are shown in Table 4-2.

Table 4-2. Calculation of vertical shear stresses on the canister surface for base case 2

Total force on the canister bottom	12 989 kN
Total force on the canister top	2 917.1 kN

The difference in force is taken by shear forces on the canister surface, which are generated by shear stresses proportional to the normal stresses

Total shear force	10 071 kN
Total horizontal (normal) force on the canister envelope surface	146 483 kN
Mobilized friction between the canister surface and the bentonite ($\tan\phi$)	0.0688
Shear stress in the top: $\tau_2 = \sigma_2 \cdot \tan\phi$	232 kPa
Shear stress in the bottom: $\tau_1 = \sigma_1 \cdot \tan\phi$	1 031 kPa

The mobilised friction between the canister surface and the bentonite 0.0688 corresponds to a friction angle of $\phi = 3.94^\circ$, which also is lower than the friction angle at failure and thus can be mobilised.

Alternative cases 1 and 2

Even worse cases may appear if a high density in the bottom is combined with a low density a short distance upwards due to rock fallout, which results in a strong vertical density and swelling pressure gradient. However, the density gradient has a limit, which is set by the friction angle and if this limit is exceeded there will be a homogenisation of the buffer. The worst case can thus be settled and corresponds to a friction angle of about $\phi=10^\circ$, which is the friction angle of MX-80 at high densities.

For this case the same type of calculations have been done for MX-80 and MX-80Ca. The difference is that the maximum and minimum shear stresses are known ($\tau=\sigma \cdot \tan(10^\circ)$) but the axial length along which the loss in shear stress acts is unknown and determined by axial force equilibrium with the assumption that the shear stress is only acting where there is a swelling pressure gradient. Figures 4-2 and 4-3 show the results.

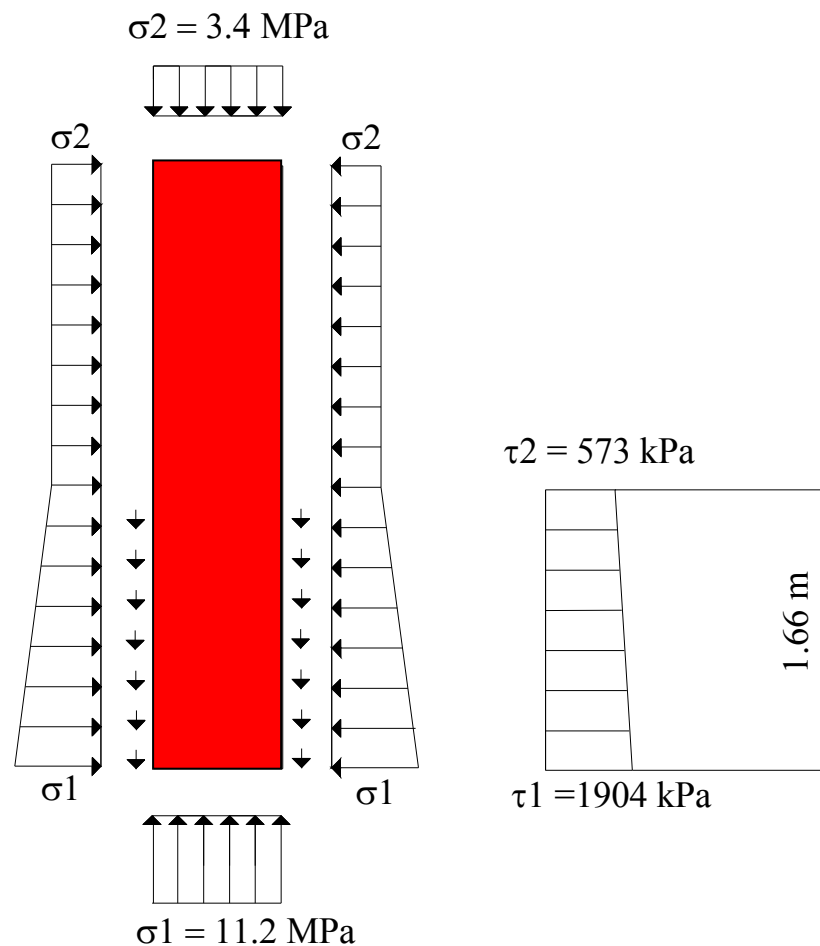


Figure 4-2. Alternative case 1. Stresses on the canister for MX-80

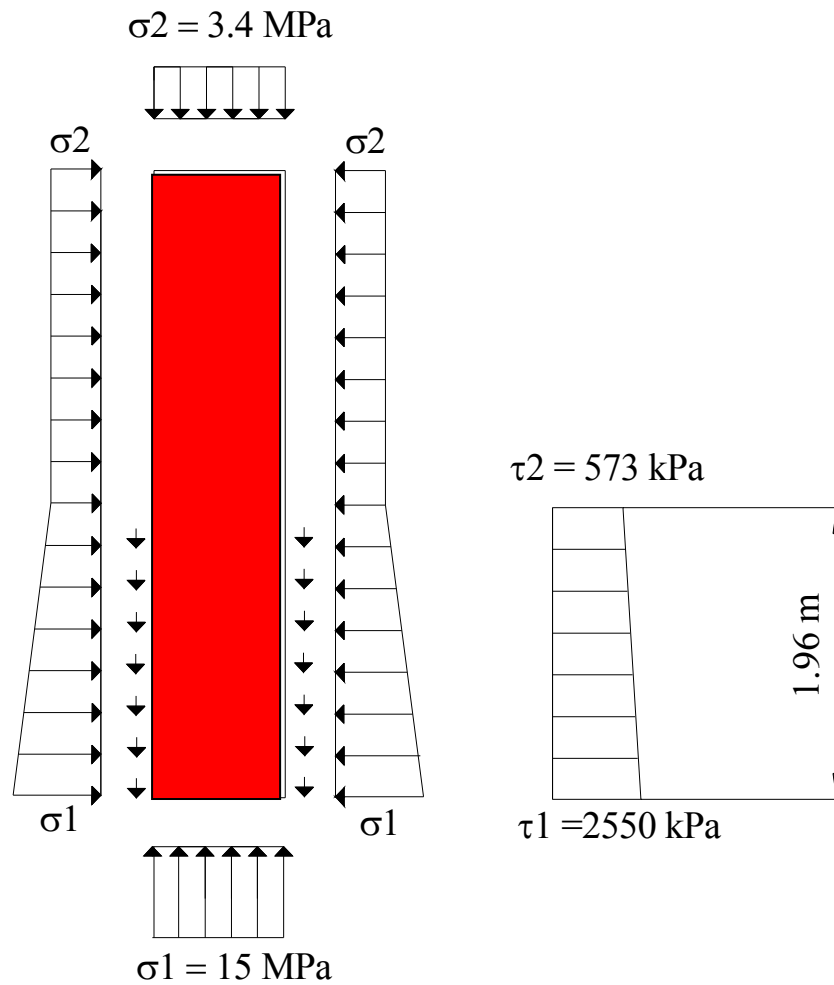


Figure 4-3. Alternative case 2. Stresses on the canister for MX-80Ca

4.3 Comments

The presented load cases are simplifications and represent a selection of the worst cases but there are of course other possible combinations. If the stresses are considered critical for the copper shell more relevant finite element calculations should be considered.

5 Conclusions and comments

A number of different load cases that may be harmful for the canister have been investigated. Such load cases are derived from uneven swelling pressure in the buffer material, both during the water saturation phase and after full water saturation. Different cases are critical for the cast iron insert and the copper shell. The irregularities that may occur in the contour of the deposition hole are taken from the Underground openings construction report /SKB, 2009b /. Simple interpretations of those data and addition of cases may yield unrealistic and thus conservative load cases. No evaluation of the quality and probability of the load cases have been done.

This report is a load definition report and the stress estimates made here are only indicative. The actual stress calculations and the assessment of acceptability are made later in separate report using 3D-FEM-modelling and taking into account shear deformation, large displacements and non-linear material properties.

Three main types of load combinations have been considered.

Remaining stresses after full water saturation of the buffer that are critical to the cast iron insert

The load cases for permanent stresses critical for the cast iron insert are derived from uneven horizontal stresses where the canister acts as a freely supported beam. The worst case that may occur if requirements on the buffer and deposition hole are fulfilled is case 1+2a, which combines a banana shaped hole and a local rock fall out of 3.75%. Simplified calculations of the stresses in the canister insert yield a maximum bending stress $\sigma_b = 111.5$ MPa.

Temporary stresses during the water saturation phase of the buffer that are critical to the cast iron insert

The load cases are for temporary stresses also derived from uneven horizontal stresses where the canister acts as a freely supported beam. The worst case that may occur if requirements on the buffer and deposition hole are fulfilled is case 1, which is caused by a banana shaped hole. Simplified calculations of the stresses in the canister insert yield a maximum bending stress $\sigma_b = 105$ MPa.

The load case is the result of simplified assumptions during the complicated wetting phase and is probably conservative.

Remaining stresses after full water saturation of the buffer that are critical to the copper shell

The most critical stresses on the copper shell may proceed from uneven vertical stresses caused by vertical density gradients in the buffer, which causes shear stresses on the copper. The worst case comes from a high buffer density of Ca converted MX-80 in the bottom of the deposition hole in combination with unconverted MX-80Na in the upper part and the highest possible axial density gradient caused by rock fallout. This case yields axial shear stresses on the copper shell that is linearly reduced from $\tau = 2.55$ MPa to $\tau = 0.573$ MPa over the length 1.96 m.

The complicated nature of these load cases calls for more relevant finite element calculations if the stresses are considered critical.

6 References

Andersson C, Johansson Å, 2002. Boring of full scale deposition holes at the Äspö Hard Rock Laboratory. Operational experiences including boring performance and a work time analysis. SKB TR-02-26. Svensk Kärnbränslehantering AB.

Börgesson L, Johannesson L.-E, Sandén T, Hernelind J, 1995. Modelling of the physical behaviour of water saturated clay barriers. Laboratory tests, material models and finite element application. SKB TR-95-20. Svensk Kärnbränslehantering AB.

Börgesson L, Dueck A, Johannesson L-E, 2009. Material model for shear of the buffer. Evaluation of laboratory test results. SKB-doc 1223374. Svensk Kärnbränslehantering AB.

SKB, 2009a. Design, production and initial state of the buffer for the safety assessment SR-Site. SKB-doc 1177185. Svensk Kärnbränslehantering AB.

SKB, 2009b. Design, construction and initial state of the underground openings for the safety assessment SR-Site. SKB-doc 1177188. Svensk Kärnbränslehantering AB.